[10] R. Snyder, "New application of evanescent mode waveguide to filter design," *IEEE Trans. Microwave Theory Tech.*, Dec. 1977.
[11] —, "Broadband waveguide or coaxial filters with wide stopbands, using a stepped-wall evanescent mode approach," *Microwave J.*, Dec. 1983.
[12] MATHCAD, by MATHSOFT, Cambridge, MA.

Analysis and Modeling of Coupled Dispersive Interconnection Lines

T. Dhaene, S. Criel, and D. De Zutter

Abstract—**In this short paper, we present a standard method for the analysis and the simulation of coupled dispersive interconnection structures. A high-frequency circuit model is proposed which is well-suited for CAD applications. A lot of attention is paid to the physical interpretation of the full-wave parameters.**

Introduction

A large number of publications deal with the calculation of the hybrid-mode characteristics of coupled interconnection structures. The general waveguide structure with N propagating fundamental modes is completely characterized by $N(N + 1)$ complex frequency dependent parameters. These parameters can be the N^2 line-mode characteristic impedances Z_{ip} and the N modal propagation factors γ_p which follow directly from the full-wave analysis. Quite often, the meaning of the so-called "line-mode characteristic impedance" Z_{ip} (associated with conductor i and eigenmode p) is misunderstood and there is some confusion between this line-mode characteristic impedance and the circuit-oriented characteristic impedance matrix $\boldsymbol{Z}_c$, which relates the circuit voltages and currents. This can lead to incorrect calculations and wrong interpretations.

Until now, the full-wave data are not often used for transient simulation [1]–[2]. In this paper a high-frequency circuit model is presented for the simulation of coupled dispersive interconnection structures. A frequency dependent circuit model is required if the dispersive nature of such a structure has to be taken into account. A simple two-line system, earlier described by Fukuoka *et al.* [3], is used as typical example. Emphasis is on the application and interpretation of the circuit model. The complete theoretical background of the model is presented elsewhere [4]. Based on the correct interpretation of the line-mode impedance and the circuit impedance, a new and to our understanding more correct physical interpretation of the different relevant parameters is given.

Full-Wave Circuit Model

Consider a general multiconductor transmission line structure with N conductors and a reference conductor. For such hybrid interconnection structures, the conductor voltages $\boldsymbol{V}_C(z)$ and currents $\boldsymbol{I}_c(z)$ cannot be calculated in an unambiguous way as line-integrals of the electric and magnetic fields. $\boldsymbol{V}_c$ is a vector consisting of elements $V_{ci}(i = 1, \cdots, N)$ where V_{ci} is the circuit voltage associated with conductor i. $\boldsymbol{I}_c$ is defined in an analogous way. Only in the quasi-static limit, both circuit parameters, voltage and current, have a unique and clear circuit interpretation.

We use the well-accepted *PI-formulation* [4]–[5] to model the structure under study. This approach is well-suited for microstrips, striplines and related structures. The circuit current $I_{ci}(z)$ is chosen to be identical to the total longitudinal current flowing along conductor i. Furthermore, both the circuit model and the real waveguide structure are required to have the same complex modal propagation factors and to propagate the same average complex power. This leads to the generalized frequency dependent telegrapher's equations:

$$-\frac{d}{dz}\boldsymbol{V}_c(z, \omega) = j\omega \boldsymbol{L}(\omega)\boldsymbol{I}_c(z, \omega) \quad (1a)$$

$$-\frac{d}{dz}\boldsymbol{I}_c(z, \omega) = j\omega \boldsymbol{C}(\omega)\boldsymbol{V}_c(z, \omega) \quad (1b)$$

where $\boldsymbol{L}(\omega)$ and $\boldsymbol{C}(\omega)$ are the generalized N *by* N inductance and capacitance matrices respectively.

In the quasi-static approximation $\boldsymbol{L}$ and $\boldsymbol{C}$ are frequency independent [6]. In [4] it is shown how this quasi-static concept can be extended to cover the full-wave case. As announced in the introduction, we will not go into detail at this point but we will use a relevant example to clarify the concept in relation to previously-published results. It has to be emphasized that (1a) and (1b) are well-suited for CAD applications precisely because they formulate the multiconductor transmission line problem in terms of the familiar telegrapher's equations.

The frequency dependent characteristic impedance matrix $\boldsymbol{Z}_c(\omega)$ is also very useful for circuit simulation. It follows directly from (1):

$$\boldsymbol{Z}_c(\omega) = [\boldsymbol{L}(\omega)\boldsymbol{C}(\omega)]^{-0.5}\,\boldsymbol{L}(\omega). \quad (2)$$

This real, symmetric N by N matrix is defined in an unambiguous way and can be seen as the input impedance matrix of the infinitely long coupled transmission line structure. The characteristic impedance matrix relates the circuit current waves to the circuit voltage waves traveling in positive longitudinal direction.

Discussion of the Circuit Model—Example

Now, we analyze a representative asymmetric interconnection structure which was originally described by Fukuoka *et al.* [3]. Fig. 1(a) shows the cross-section of the coupled two-line system. The lines are embedded in an inhomogeneous medium. The structure consists of a perfectly conducting reference conductor, a silicon dioxide layer (SiO_2, $\epsilon_r = 4$) of 20 μm high, and a half-infinite top-layer (air, $\epsilon_r = 1$). The width of both strips is 10 μm. Horizontally, the two strips are separated by 30 μm.

In this structure two fundamental modes can propagate: a c-mode and a π-mode. The longitudinal currents flowing along the conductors are in phase for the c-mode, and in anti-phase for the π-mode. The c-mode corresponds to the even mode in a symmetric structure, while the π-mode corresponds to the odd mode. Note that no even or odd modes can exist in an asymmetrical coupled interconnection structure. In [3], the c- and π-mode seem to be interchanged.

Manuscript received November 19, 1991; revised May 1, 1992. This work was supported by a grant to the first author from the IWONL (Instituut tot Aanmoediging van het Wetenschappelijk Onderzoek in de Landbouw en de Nijverheid) and by a grant to S. Criel from the NFWO (National Fund for Scientific Research of Belgium). D. De Zutter is Senior Research Associate for the NFWO.
The authors are with the Laboratory of Electromagnetism and Acoustics, University of Ghent, Sint-Pietersnieuwstraat 41, 9000 Ghent, Belgium.
IEEE Log Number 9202904.

0018-9480/92$03.00 © 1992 IEEE

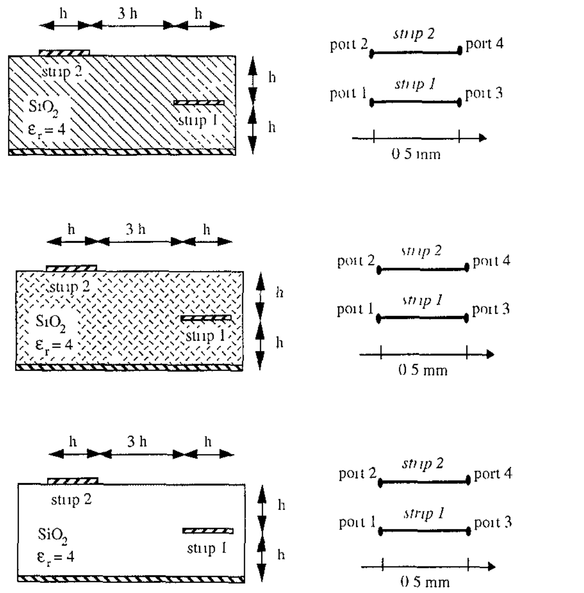

Fig. 1. (a) Cross-section of a non-coplanar strip configuration with $h = 10\ \mu$m. (b) Network configuration.

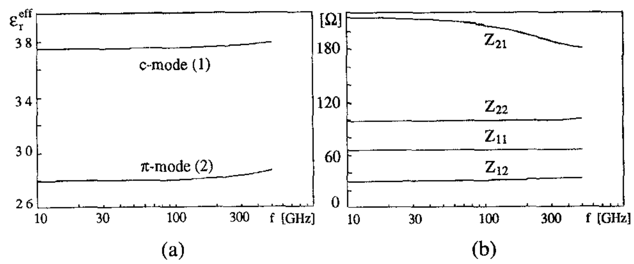

Fig. 2. (a) Effective dielectric constant of c- and π mode, (b) line-mode characteristic impedances.

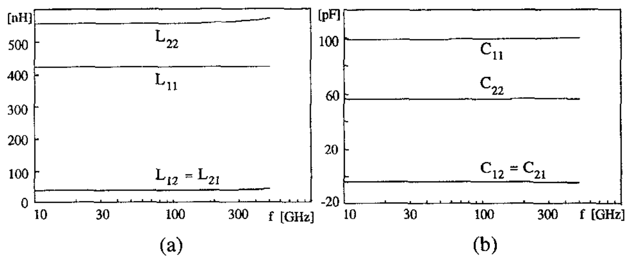

Fig. 3. Elements of the (a) inductance matrix, (b) capacitance matrix.

The electric field of the π-mode (mode 2) spreads more into the upper layer ($\epsilon_r = 1$) as compared to the field of the c-mode (mode 1) which is mainly confined to the substrate ($\epsilon_r = 4$). Hence, the effective dielectric constant of the π-mode will be lower than the effective dielectric constant of the c-mode, and the propagation velocity of the c-mode will be smaller than the one of the π-mode. Owing to the dielectric conductance, the electromagnetic fields concentrate more and more in the substrate as the frequency increases, and the effective dielectric constants increase slightly.

Using the space-domain Green's function approach [7], the effective dielectric constants (Fig. 2.a) and the line-mode characteristic impedances (Fig. 2(b)) are calculated in the frequency range 10 GHz–500 GHz. The frequency dependent behaviour of the effective dielectric constants can easily be understood as explained above. The line-mode characteristic impedance $Z_{ip}(i, p = 1, 2)$ associated with conductor i and eigenmode p is defined as the ratio of the circuit voltage V_{ip} to the circuit current I_{ip} associated with mode p and propagating in the longitudinal direction along transmission line i [5], thus:

$$Z_{ip} = \frac{V_{ip}}{I_{ip}}. \tag{3}$$

These line-mode characteristics impedances are defined in a unique way, but they are less suited for circuit simulation. It are also these impedances which are used in [3]. They are defined in a slightly different way by Jansen [8].

The generalized symmetric inductance $\boldsymbol{L}(\omega)$ and capacitance $\boldsymbol{C}(\omega)$ matrices are much more suited for CAD applications than the effective dielectric constants and the line-mode characteristic impedances.

The lossless hybrid two-line structure is completely characterized by 3 generalized inductance (L_{11}, L_{22}, $L_m = L_{21} = L_{12}$) and 3 generalized capacitance (C_{11}, C_{22}, $C_m = C_{21} = C_{12}$) parameters (see Fig. 3). These parameters can easily be interpreted, starting from their well-known physical meaning at low frequencies and by simply inferring from the curves on the figure how their value evolve as a function of frequency. The quasi-static inductance and capacitance matrices are respectively:

$$\boldsymbol{L} = \begin{bmatrix} 421.6 & 39.6 \\ 39.6 & 555.9 \end{bmatrix} \text{nH/m} \tag{4a}$$

and

$$\boldsymbol{C} = \begin{bmatrix} 99.1 & -4.1 \\ -4.1 & 56.5 \end{bmatrix} \text{pF/m} \tag{4b}$$

At frequencies higher than 100 GHz the frequency dispersion becomes important. In many practical applications, the small difference between the full-wave and the quasi-static parameters may not be important. Note that a full-wave analysis is required to conclude this!

Fig. 4 shows the elements $Z_{cij}(i, j = 1, 2)$ of the frequency dependent characteristic impedance matrix $\boldsymbol{Z}_c(\omega)$ defined in (2).

Using the full-wave data of Figs. 2, 3, and 4, we have calculated some relevant network parameters of the two-line system. As in the original example, the length of both strips is chosen to be 0.5 mm. This network is represented in Fig. 1(b). Thanks to the symmetry and the reciprocity of the structure, several S-parameters are equal, such as S_{11} and S_{33}, S_{12} and S_{34}, etc. As an example, the amplitudes of some of the elements of the scattering parameter matrix (reference impedance = 50 Ω) are shown in Fig. 5.

With an excitation of the first conductor (in the middle of the substrate) corresponds an electromagnetic field that is mainly concentrated in the dielectric substrate. The field associated with an excitation of the second conductor (at the air-substrate interface) is much more concentrated in the top-layer. On the other hand, we know that the π-mode generates a larger electric field in the top layer than the c-mode. So we expect that the main contribution to the field associated with the first (second) conductor is caused by the c- (π-) mode. This is confirmed by the following line-mode relations: $|V_{11}| \gg |V_{12}|$, $|V_{22} \gg |V_{21}|$, $|I_{11}| \gg |I_{12}|$ and $|I_{22}| \gg |I_{21}|$.

Owing to the weak coupling of both strips, the line-mode char-

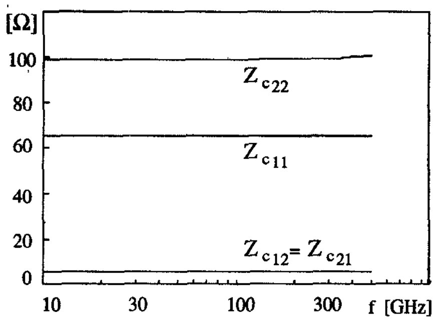

Fig. 4. Elements of the characteristic impedance matrix.

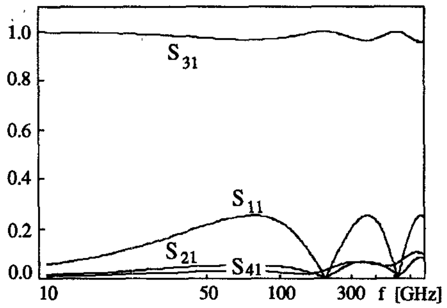

Fig. 5. Elements of the scattering parameter matrix.

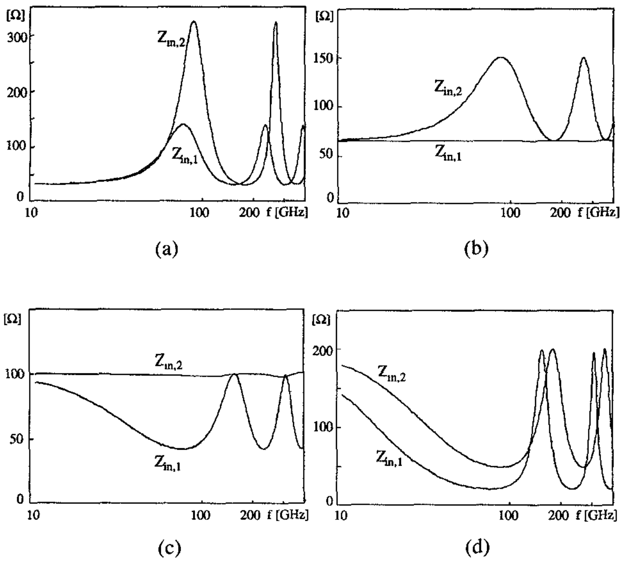

Fig. 6. Real part of input impedances of both strips. (a) 30 Ω. (b) 65 Ω, (c) 100 Ω, (d) 200 Ω-terminations.

acteristic impedances Z_{11} and Z_{22} (Fig. 2(b)) correspond very well with the diagonal elements of the characteristic impedance matrix $\mathbf{Z}_c(\omega)$ (Fig. 4) as expected. Both transmission lines are quasi-matched if the lines are terminated by $Z_{c11}(\approx 65\ \Omega)$ and Z_{c22} (≈ 100 Ω), or by Z_{11} and Z_{22}, respectively.

We have calculated the frequency dependent input impedance at a port if all other ports of the circuit are terminated by a specific impedance [9]. In Fig. 6, the real parts of the input impedances of both lines are shown for different terminating impedances (30 Ω, 65 Ω, 100 Ω and 200 Ω). $Z_{in,i}$ refers to the input impedance seen at port i. As expected, the input impedance of the first and the second line is nearly constant over the whole frequency range if both lines

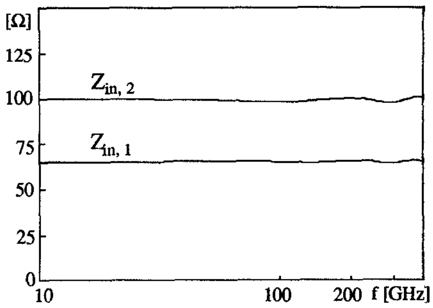

Fig. 7. Real part of input impedances of both strips if all ports are quasi-matched i.e. first strip terminated by a 65 Ω resistor and second strip terminated by a 100 Ω resistor.

are terminated by 65 Ω ($\approx Z_{c11}$) and 100 Ω ($\approx Z_{c22}$) respectively. The transmission line structure is then quasi-matched (Fig. 7).

Fukuoka *et al.* [3] use the line-mode characteristic impedances $Z_{ip}(\omega)\,(i, p = 1, 2)$ instead of the circuit characteristic impedances $Z_{cij}(\omega)\,(i, j = 1, 2)$ for all circuit calculations. This leads to completely different conclusions and to other calculation results. Our results are based on a new and to our understanding correct physical interpretation of the different relevant parameters.

Conclusion

In this paper, a circuit-oriented frequency dependent characteristic impedance matrix $\mathbf{Z}_c(\omega)$ is defined together with the generalized frequency dependent telegrapher's equations. A standard method for the analysis and the simulation of coupled dispersive interconnection structures is presented. The new high-frequency circuit description is well-suited for simulation and CAD applications.

References

[1] T. Dhaene and D. De Zutter, "Extended scattering matrix approach for transient analysis of coupled dispersive lossy transmission lines with arbitrary loads," *Electromagnetics*, no. 1, 1993, accepted for publication.

[2] L. Carin and K. J. Webb, "An equivalent circuit model for terminated hybrid-mode multiconductor transmission lines," *IEEE Trans. Microwave Theory Tech.*, vol. 37, no. 11, pp. 1784–1793, Nov. 1989.

[3] Y. Fukuoka, Q. Zhang, D. P. Neikirk, and T. Itoh, "Analysis of multilayer interconnection lines for a high-speed digital integrated circuit," *IEEE Trans. Microwave Theory Tech.*, vol. MTT 33, no. 6, pp. 527–532, June 1985.

[4] T. Dhaene and D. De Zutter, "CAD-oriented general circuit description of uniform coupled lossy dispersive waveguide structures," *IEEE Trans. Microwave Theory Tech.*, vol. 40, no. 7, pp. 1545–1559 (special issue on Process-Oriented Microwave CAD and Modeling, July 1992.

[5] N. Faché and D. De Zutter, "New high-frequency circuit model for coupled lossless and lossy waveguide structures," *IEEE Trans. Microwave Theory Tech.*, vol. 38, no. 3, pp. 252–259, Mar. 1990.

[6] I. V. Lindell, "On the quasi-TEM modes in inhomogeneous multiconductor transmission lines," *IEEE Trans. Microwave Theory Tech.*, vol. MTT-29, no. 8, August 1981, pp. 812–817.

[7] N. Faché and D. De Zutter, "Circuit parameters for single and coupled microstrip lines by rigourous full-wave space-domain analysis," *IEEE Trans. Microwave Theory Tech.*, vol. 37, no. 2, pp. 421–425, Feb. 1989.

[8] R. H. Jansen, "Unified user-oriented computation of shielded, covered and open planar microwave and millimeter-wave transmission-line characteristics," *Microwaves, Optics and Acoustics*, vol. 3, pp. 14–22, Jan. 1979.

[9] S. Criel, "Signal propagation on multiconductor transmission lines," (in Dutch) M. Sc. thesis, University of Ghent RUG-LEA, May 1991.